

Multi-Year Vector Dynamic Time Warping Based Crop Mapping

Mustafa Teke ^{1,2*} and Yasemin Yardımcı ²

¹ Scientific and Technological Research Council of Turkey (TÜBİTAK) Space Technologies Research Institute (UZAY), Ankara, Turkey; mustafa.teke@tubitak.gov.tr

² Informatics Institute, Middle East Technical University, Ankara, Turkey; yyardim@metu.edu.tr

* Correspondence: mustafa.teke@tubitak.gov.tr

Received: date; Accepted: date; Published: date

Abstract: Recent automated crop mapping via supervised learning-based methods have demonstrated unprecedented improvement over classical techniques. However, most crop mapping studies are limited to same-year crop mapping in which the present year's labeled data is used to predict the same year's crop map. Classification accuracies of these methods degrade considerably in cross-year mapping. Cross-year crop mapping is more useful as it allows the prediction of the following years' crop maps using previously labeled data. We propose Vector Dynamic Time Warping (VDTW), a novel multi-year classification approach based on warping of angular distances between phenological vectors. The results prove that the proposed VDTW method is robust to temporal and spectral variations compensating for different farming practices, climate and atmospheric effects, and measurement errors between years. We also describe a method for determining the most discriminative time window that allows high classification accuracies with limited data. We carried out tests of our approach with Landsat 8 time-series imagery from years 2013 to 2016 for classification of corn and cotton in the Harran Plain, and corn, cotton, and soybean in the Bismil Plain of Southeastern Turkey. In addition, we tested VDTW corn and soybean in Kansas, the US for 2017 and 2018 with the Harmonized Landsat Sentinel data. The VDTW method achieved 99.85% and 99.74% overall accuracies for the same and cross years, respectively with fewer training samples compared to other state-of-the-art approaches, i.e. spectral angle mapper (SAM), dynamic time warping (DTW), time-weighted DTW (TWDTW), random forest (RF), support vector machine (SVM) and deep long short-term memory (LSTM) methods. The proposed method could be expanded for other crop types and/or geographical areas.

Keywords: Time series; phenology; multi-year classification; dynamic programming; Landsat; crop mapping; land use; corn; cotton; soybean

1. Introduction

The world population is expected to exceed nine billion in 2050 [1]. Providing adequate nutrition for the increasing human population is a significant concern. Advanced agricultural technologies, such as precision agriculture and precision irrigation are rapidly emerging to optimize water, fertilizers, and pesticides; thereby enabling higher crop yield. Accurate crop maps are the first requirements of advanced agriculture applications such as yield forecasting. Early-season crop yield estimates are a crucial factor for food security and monitoring agricultural subventions. Crop maps are also an essential tool for statistical purposes to analyze annual changes in agricultural production. However, there are a variety of field crops with similar phenologies and spectral signatures. Likewise, the same plant may have different growing periods in different regions. These properties of field crops render crop mapping a challenge in classification.

Due to the importance of crop mapping on a global scale, various organizations focus on crop monitoring [2]. One of the most notable examples of crop mapping systems is CropScape. CropScape

enables the United States Department of Agriculture (USDA) to map crops in the US for statistical purposes. Governments ensure food security via allocating agricultural subsidies such as LPIS in EU and Turkey [3].

Field surveys are the most basic method of crop mapping. However, they are expensive and may not cover all fields [4]. Furthermore, crop field surveying is prone to human errors [5]. An effective multi-year crop mapping methodology is required to monitor the status of crops, verify and monitor subventions, forecast crops, ensure price stability and obtain agricultural statistics. Remote sensing is a critical technology that would allow us mapping of field crops by using aerial and satellite imagery from various sources. Crop mapping methods may use single, multi-temporal and time-series satellite imagery. These algorithms typically require field data collection for each year of interest. On the other hand, cross-year crop mapping enables the use of previous field surveys for the present year, thereby reducing the effort required for the collection of training samples.

We surveyed multi-temporal and time-series crop mapping literature with an emphasis on cross-year crop mapping. Land use/land cover (LULC) is an extensively studied research area [6–8]. Moreover, crop mapping is a sub-research area of LULC. Multi-temporal and time-series electro-optical satellite imagery were used in the majority of the studies in crop mapping that we surveyed. Multi-temporal images, which are less frequently acquired than time-series imagery, were also commonly used in crop mapping studies. Özdarıcı-Ok and Akyürek developed a method for segment-based classification of multi-temporal Electro-optic and SAR images in Karacabey, Bursa, Turkey [9,10]. An object-oriented multi-temporal crop classification method for four Landsat 7 ETM+ images of 2012 in Montana, USA was used with an RF classifier to discriminate cereal, pulse, and other classes [11]. Löw et al. developed a decision fusion of decision tree (DT), RF, SVM, and multilayer perceptron (MLP) classifiers to classify multi-temporal RapidEye imagery comprised of alfalfa, cotton, fruit trees, rice, wheat, and melon [12]. A winter wheat mapping in northern China with multi-temporal and multi-sensor data was conducted and found out that the RF classifier produced higher accuracies compared to artificial neural networks (ANN), maximum likelihood (ML), and SVM [13]. These studies performed both training and testing using the same year data. Even though these studies indicated improved accuracies over single imagery, they did not present a multi-year solution due to the acquisition of sparse imagery.

Time-series data involve acquiring a large number of satellite images with high temporal frequency. Petitjean and Weber used DTW for land cover classification with 46 time-series FORMOSAT-2 images of 2006 [14]. Tatsumi et al. studied classification (alfalfa, asparagus, avocado, cotton, grape, maize, mango, and tomato) of time-series Landsat 7 ETM+ images with random forest (RF) classifier in Peru [15]. Zheng et al. used 24 time-series Landsat 5 TM and 7 ETM+ of 2010 for classification of crops in Phoenix, AZ [16]. Six single crops and three double crops were classified with SVM. Sixteen-day MODIS time-series data of 2001 was used for land use classification (urban, forest, agriculture) in the USA [17]. SVM, neural networks (NN) and classification and regression tree (CART) were compared and SVM performed better. Lunetta et al. classified wheat, corn, and cotton with MODIS time-series 16-day NDVI composite data in the Great Lake Basin, US, and Canada with a three-layer MLP classifier. In their study, crop layers of 2005-2007 were compared with USDA NASS' Cropland Data Layer (CDL) and crop ration patterns were analyzed: observed differences between CDL and their results were between 1-11.1%. Zong et al. developed a spectro-temporal crop classification method to classify corn and soybean from time-series Landsat 5 and 7 images [18]. Time-series features are extracted from the parameters of a double sigmoid curve. This study achieved 89.4% same-year (SY) accuracy and 83.4% cross-year (CY) accuracies. Maus et al. proposed time-weighted dynamic time warping (TWDTW), which is an improvement over dynamic time warping (DTW) by incorporating the time difference between samples as an additional cost [19]. In another study, pixel-based and object-based TWDTW methods were compared with random forest (RF) with Sentinel-2 time-series data. Object-based TWDTW achieved comparable results to RF classifier [20]. Massey et al. studied the multi-year distribution of major crop types in the conterminous US with time-series MODIS data between 2001 and 2014 [21]. A phenology-based decision tree approach achieved year-specific (same-year) accuracies of >78% and generalized (multi-year) accuracies > 75%

in 13 agro-ecological zones. A multi-decade and multi-sensor time series crop mapping was performed in [22] with Landsat imagery was fused with Sentinel-2 and MODIS when available. The method composed of two expert-rules and two-random forests to classify winter and summer crops in Queensland, Australia between 1987 and 2017.

A majority of the studies on multi-temporal or time-series satellite imagery crop classification did not take time into account as a feature and focused on mapping crops using same-year data for both training and validation. However, multi-year analysis enables earlier classification of crops based on previous years' data. Only a limited number of studies conducted multi-year comparisons such as [18,19]. These studies presented classification accuracies where cross-year results were considerably lower compared to same-year results, and they required a substantial amount of training samples. Even if cross-year crop mapping eliminated the necessity of yearly training sample collection, these studies still needed considerable training data. Again, most studies did not incorporate annual temporal variations in their studies; one notable exception is the work of [19]. RF and SVM were most used classifiers in crop mapping.

Furthermore, we considered deep (DL) learning methods for cross-year crop mapping. DL has gained popularity in recent years due to its applications in numerous areas [23]. Deep convolutional neural networks and recurrent neural nets were applied for crop mapping [24,25]. DL methods achieved higher classification accuracies compared to other classification methods such as SVM and RF [26]. However, DL requires a vast amount of training data and an extensive amount of computing power. The crop-mapping studies that used DL, mentioned above, were tested with only same-year data, while the majority of the data were used in training.

In this study, we aim to develop an efficient cross-year crop mapping algorithm which uses a limited number of training samples, and is resistant to annual measurement and growth variations.

The main contribution of the study is the development of a novel vector distance-based optimal time-warping algorithm (VDTW). The VDTW method overcomes difficulties in cross-year crop classification in which training and test data are selected from different years: spectral shifts due to changes in illumination at the time of observation and temporal shifts in growth due to yearly climate variations or farming practices. We simulated different cases of illumination and growth changes. Furthermore, we tested our methodology in a multi-year approach in two regions (the Bismil and the Harran Plain) with distinct cropping practices. The proposed approach requires fewer training samples compared to other methods; thus it significantly reduces the costly collection of field data.

As a second contribution of this work, we focused on the feasibility of exploiting crop phenologies to use fewer and effective image acquisitions. A method which automatically determines the optimal time window in which crops have discriminative phenological features is developed. The algorithm developed to select this optimal time allows mid-season crop classification, enabling early accurate prediction of crop yields. In this way, the necessary precautions for transport, storage as well as price volatility could be taken.

2. Study Sites and Data

2.1. Study Sites

In this study, we tested the VDTW method in two different regions: The Harran Plain and The Bismil Plain. Both regions are located in the South East of Turkey. The locations of the Harran Plain (blue) and the Bismil Plain are shown in Figure 1. The region has a Mediterranean climate with about 400-450mm yearly rainfall according to General Directorate of Meteorology of Turkey.

The Harran Plain is bordered by Şanlıurfa city and Germüş Mountains in the north, Tek Tek Mountains in the east, Akçakale town and the Syria border in the south and Fatik Mountains in the west. Its length is 65 km from north to south, and its total area is 225000 ha. According to the Turkish Statistical Institute (TÜİK) data, barley, wheat, corn, and cotton are the principal crops of the Harran Plain. The Harran Plain is irrigated by the canals from the Atatürk Dam [27,28].

The Bismil dataset covers the Bismil Plain around Bismil city in Diyarbakır County. Bismil city is located along the Tigris River. The area extends next to the border between Batman and Diyarbakır counties. Corn, cotton, soybean, and wheat are the major crops in the region.

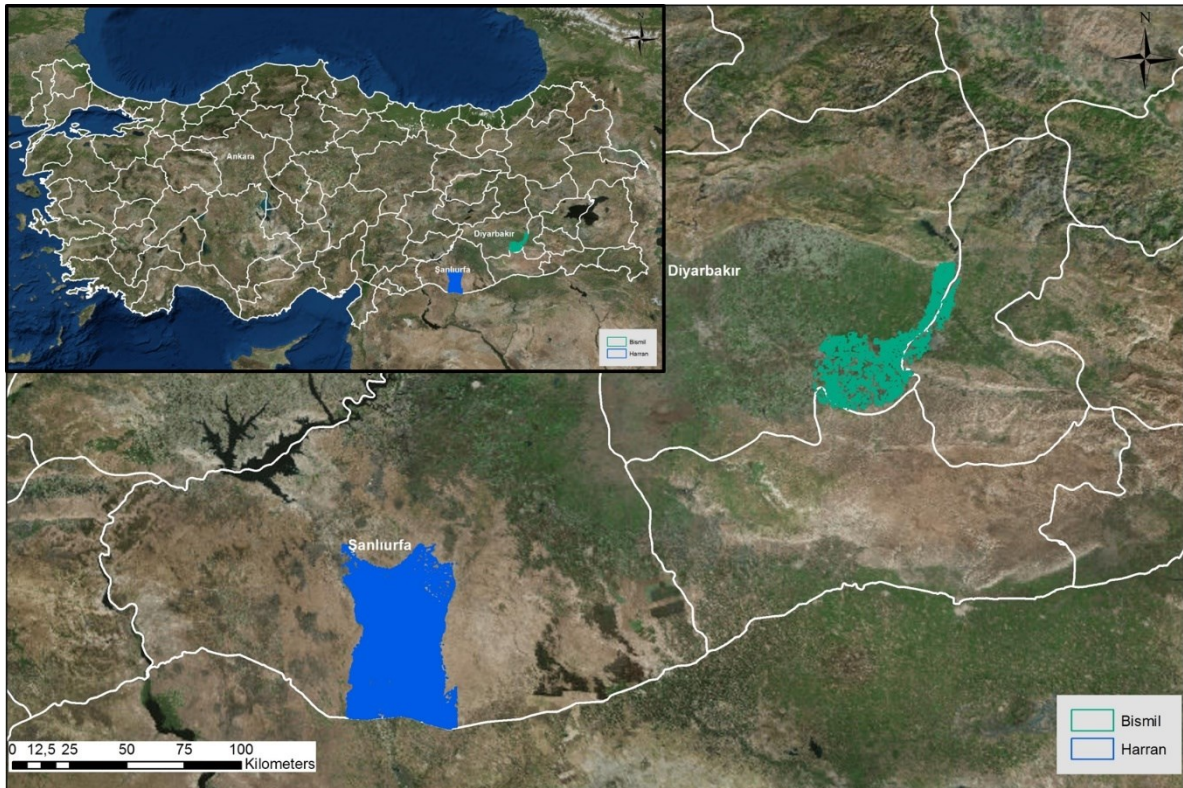


Figure 1. The Harran and The Bismil Plains are depicted in Turkey.

Our test dataset was selected from the Northeast of Kansas (Figure 2). The test area is selected as the overlap of Landsat 8 Path 28/Row 33 and Path 27/Row33 tiles also fully covered by a Sentinel-2 tile. The Kansas data set extends on Brown, Jackson, Nemaha, Shawnee, Pottawatomie, and Wabaunsee counties. Major crops in the region are corn and soybean.

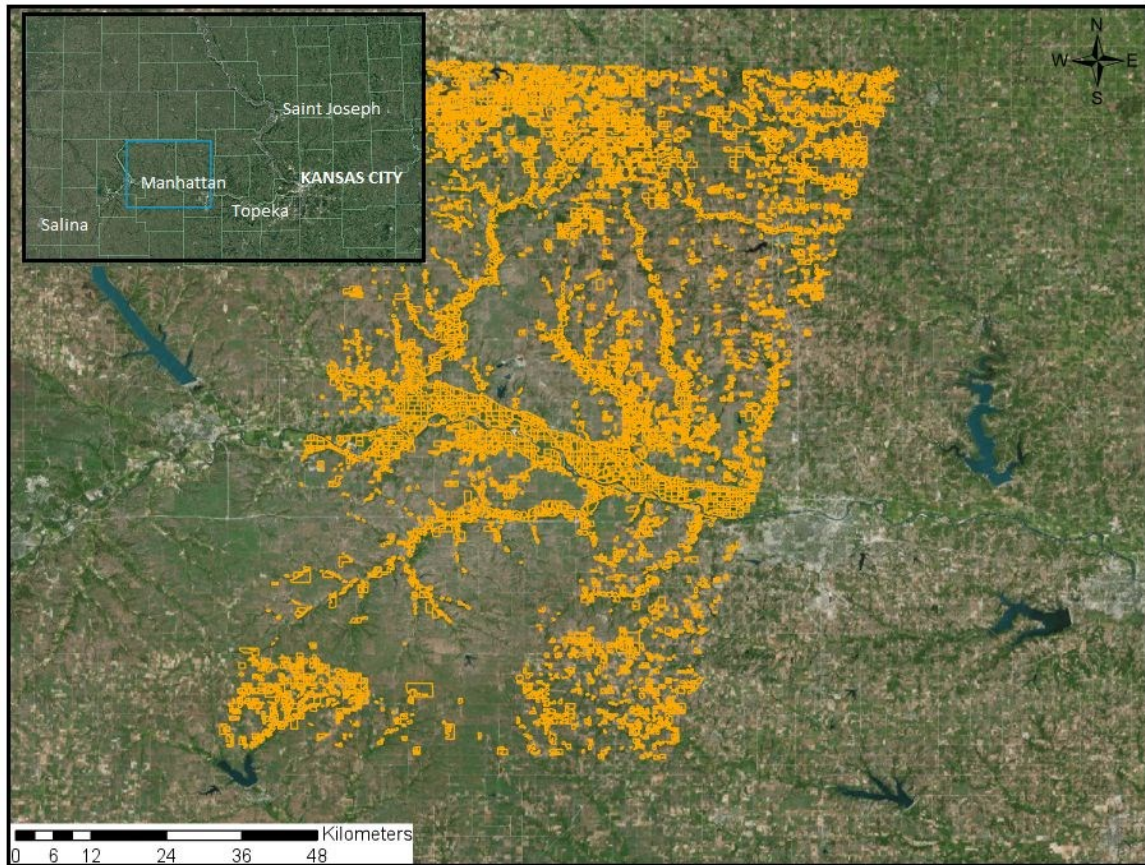


Figure 2. The Kansas dataset is depicted.

2.2. Satellite Imagery

Multi-year data of Landsat 8 satellite were used in this study. Landsat 8 covers the Earth every 16 days. Landsat 8 data were converted to surface reflectance by the U.S. Geological Survey (USGS) [29]. Harmonized Landsat Sentinel data were used for the Kansas dataset.

The imagery of the Harran Plain was from early June to the end of October. Twenty images from 2013, 2014 and 2015, and 18 images from 2016 were used. Imagery acquisition details for the Harran Plain are presented in Figure 3.

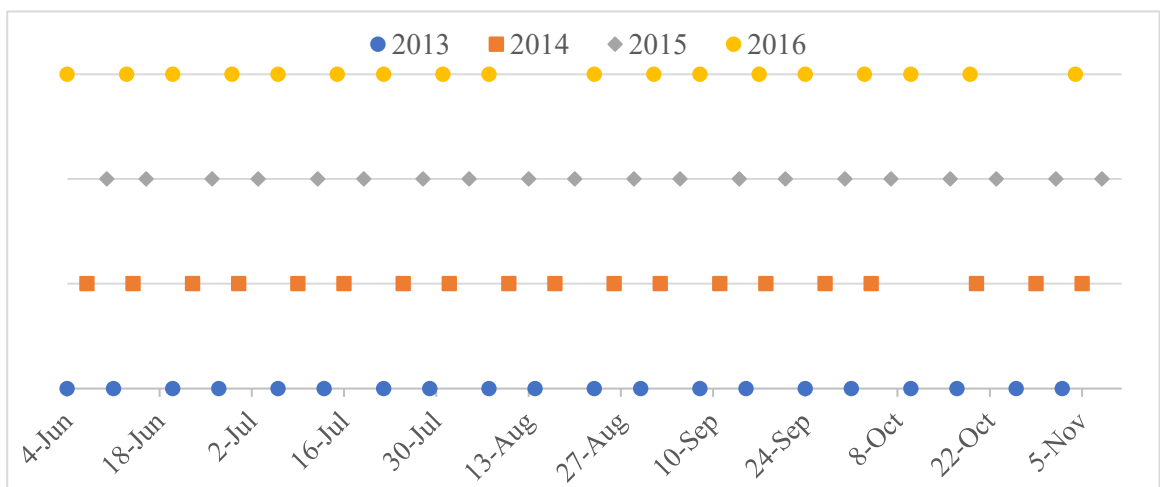


Figure 3. Landsat 8 imagery Harran dataset acquisitions dates in 2013, 2014, 2015 and 2016.

The satellite imagery from April to November was used for the Bismil Plain. The Bismil Plain dataset has 21 images in 2013 and 2014, and 19 images in 2015. The detailed information regarding images at each year is presented in Figure 4.

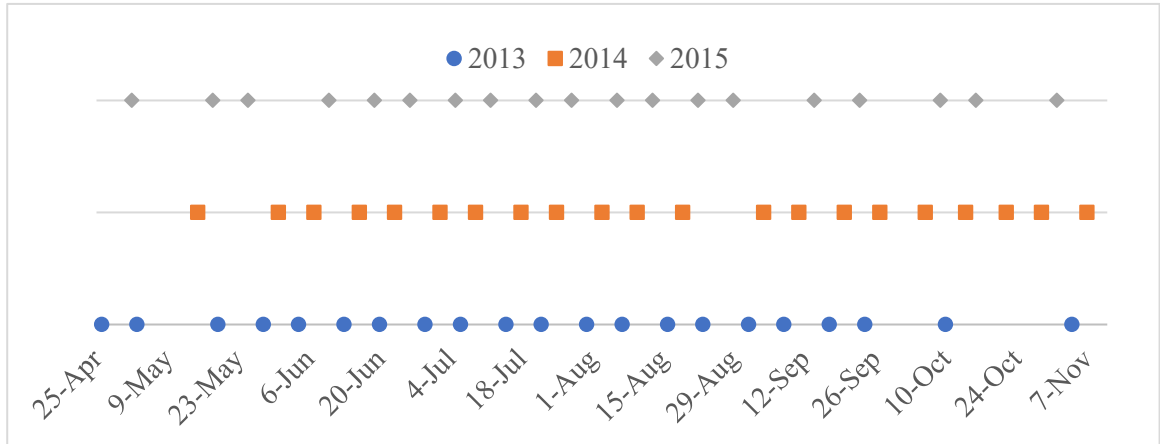


Figure 4. Landsat 8 Bismil dataset imagery acquisitions dates in 2013, 2014, and 2015.

We used Harmonized Landsat 8 and Sentinel-2 (HLS) data for the Kansas dataset. The HLS data enabled more cloud-free data acquisitions. The Kansas data set has 22 images (15 Landsat 8 and 7 Sentinel-2) in 2017 and 22 (five Sentinel-2 and 17 Landsat 8) images in 2018. Harmonized Landsat Sentinel project resamples Sentinel-2 imagery in to match Landsat 8 in spatial and spectral properties[30].

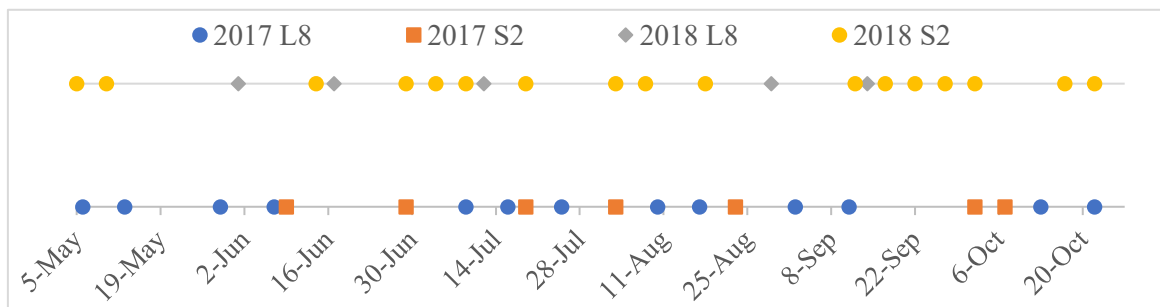


Figure 5. Landsat 8 and Sentinel-2 Kansas dataset imagery acquisition dates in 2017 and 2018.

2.3. Ground Truth Data

Ground truth is based on the Ministry of Agriculture and Forestry's National Registry of Farmers (NRF, Turkish: Çiftçi Kayıt Sistemi, ÇKS) for Turkey. In the NRF, farmers declare the crops they will grow at the start of the season and redeclare the crops they grew at the end of the season, in order to apply for government agricultural subsidies [31]. On the other hand, the ground truth of the Kansas dataset is based on USDA NASS's the Cropland Data Layer (CDL). The CDL data was created based on USDA's Farm Services Agency (FSA) Common Land Unit (CLU) data.

The NRF contains vectors of agricultural fields. Figure 6 depicts the ground truth. The samples in the north and southwest of the Harran Plain are excluded from the study because those lands are not consolidated and there is a mismatch between the NRF data and field observations. Furthermore, some large fields grow multiple crops but declared only one of them in the NRF data. Regarding the GT, we started with census data: the declaration from the National Registry of Farmers. Then we excluded fields with multiple declarations. *In the case of Kansas dataset, we used CLU 2008 data as field boundaries.*

Ground truth errors tend to occur in the field boundaries[32] since those pixels contain mixed values of neighboring land use classes. Landsat 8 has a spatial resolution of 30 meters and images acquired at different times may have up to 24 meters positional accuracy. We applied a buffer of 50 meters to reduce edge effects and registration errors between scenes acquired on different dates. The field vectors were geolocated to overlap with the satellite images to reduce digitization and coordinate system differences. For these reasons, fields that are smaller than 5 ha were excluded from this study since elongated fields with width less than 100 meters either vanished or thinned for central median sample computation.

The median vegetation index (VI) time-series vector data of each field is assigned as a sample in the tests. A summary of the characteristics the Harran Dataset is presented in Table 1, the Bismil Dataset in Table 2, and the Kansas dataset is depicted in Table 3.

Table 1. Number, percentage distribution and areas of corn and cotton fields in the Harran dataset in 2013, 2014, 2015 and 2016

		#Fields	%Samples	Area (ha)
2013	Corn	1167	22.23	6721
	Cotton	4083	77.77	24577
	Total	5250		31298
2014	Corn	722	13.56	4080
	Cotton	4601	86.44	26875
	Total	5323		30954
2015	Corn	824	19.35	4948
	Cotton	3435	80.65	21828
	Total	4259		26776
2016	Corn	392	9.48	1602
	Cotton	3745	90.52	23921
	Total	4137		25523

Table 2. Number, percentage distribution, and areas of corn, cotton and soybean fields in the Bismil dataset in 2013, 2014 and 2015

		#Fields	%Samples	Area (ha)
2013	Corn	674	61.38	8887
	Cotton	347	31.60	3991
	Soybean	77	7.02	238
	Total	1098		13116
2014	Corn	721	54.91	11606
	Cotton	438	33.36	5115
	Soybean	154	11.73	312
	Total	1313		17033
2015	Corn	793	64.37	11842
	Cotton	349	28.33	2580
	Soybean	90	7.30	271
	Total	1232		14693

Table 3. Number, percentage distribution and areas of corn and soybean fields in the Kansas dataset in 2017 and 2018

		#Fields	%Samples	Area (ha)
2017	Corn	1167	41.66	67952
	Cotton	4083	58.34	89479
	Total	5250		157431
2018	Corn	2307	42.99	71714
	Cotton	3059	57.01	86913
	Total	5366		158627

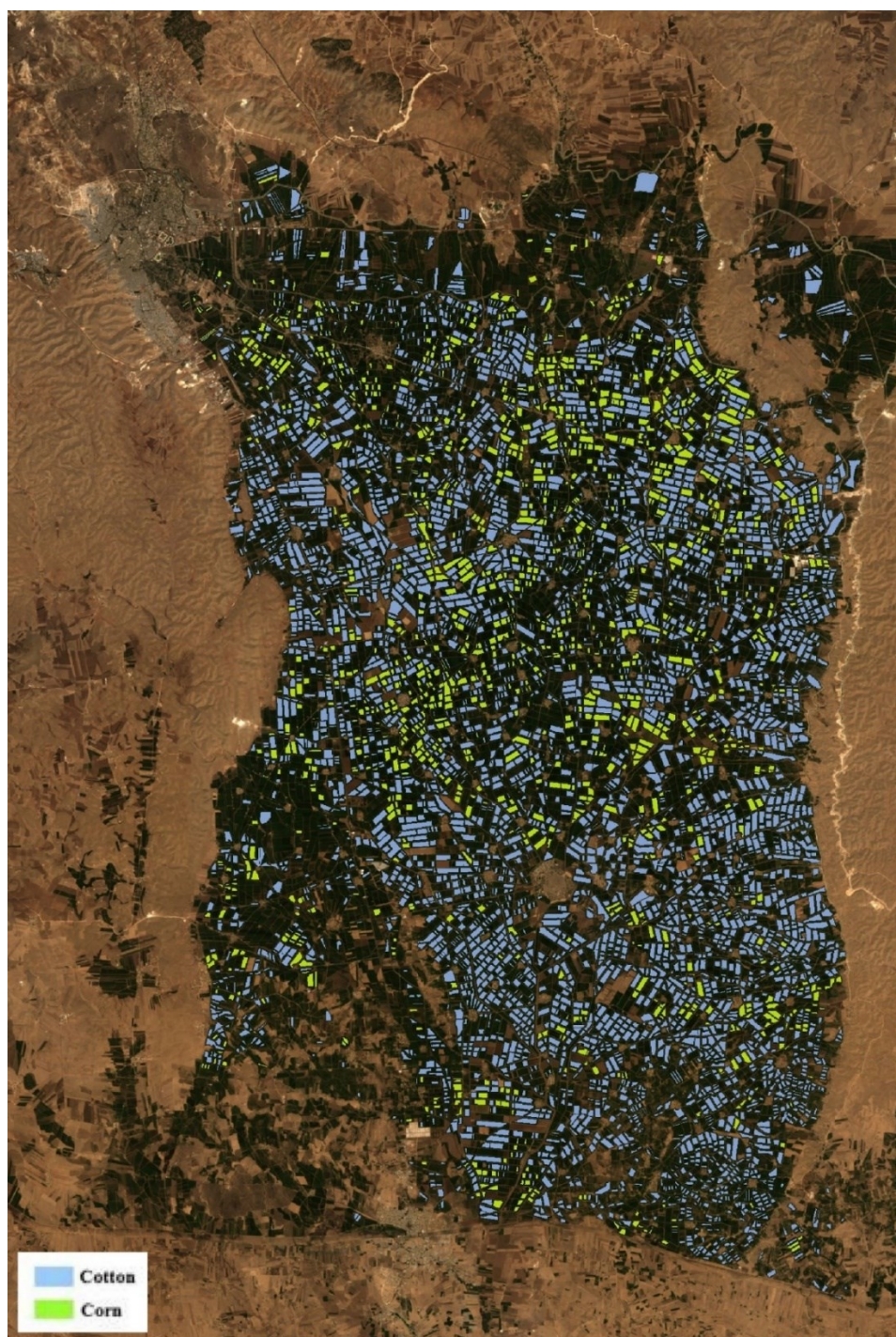


Figure 6 The Harran Plain 2013 Dataset: distribution corn and cotton fields. The fields (in the west of the Harran Plain) which are not overlapped by both WRS-2 Path 172 and 173 were excluded in the study.

3. Methods

3.1 Phenological Crop Classification

Growth and status of the crops are measured by vegetation indices. The proposed VDTW algorithm is based on time-series vegetation phenology. Vegetation indices such as NDVI are used to measure phenology information. Both the Harran Plain and the Bismil Plain are observed at different angles since two different WRS-2 paths are overlapping them. Thus, phenology information extracted from different viewing angles was affected by the bidirectional reflectance distribution function (BRDF). Huete et al. found that the soil-adjusted vegetation index (SAVI) is resistant to BRDF effects compared to NDVI [33]. Modified soil-adjusted vegetation index (MSAVI) improves SAVI since it automates the calculation of the soil line. In this study, NDVI, SAVI, optimized SAVI (OSAVI), EVI, enhanced NDVI (ENDVI), and WDRVI were compared. MSAVI slightly improved VDTW method’s cross-year crop mapping overall accuracy by 0.05% compared to NDVI (results not shown here). Moreover, the use of MSAVI improved the cross-year overall accuracy of VDTW method in the Kansas dataset by 1.5%(EVI) to 2%(NDVI).

The crop calendars of corn, cotton, and soybean in the Harran Plain, the Bismil Plain and Kansas[34] are presented in Figure 7. Figure 8 shows variations in phenology MSAVI values of corn and cotton have high differences in their early growth periods samples in 2013 as a box plot. The growth is followed by a steady maturity period. Also, harvests of corn and cotton highly overlap: corn is harvested earlier than cotton. Median phenologies of corn and cotton are shown in Figure 9(a) for the Harran Plain in 2013. Corn is grown after the harvest of winter wheat in the Harran Plain as the second crop (double cropping). Phenologies of corn, cotton, and soybean are shown in Figure 9(b) for the Bismil Plain in 2013. Soybean is grown as the second crop after winter wheat in the Bismil Plain.

	Months	March	April	May	June	July	August	September	October	November
Harran	Corn					Sowing	Growth		Harvesting	
	Cotton		Sowing	Growth				Harvesting		
Bismil	Corn	Sowing	Growth			Harvesting				
	Cotton		Sowing	Growth				Harvesting		
	Soybean					Sowing	Growth		Harvesting	
Kansas	Corn		Sowing	Growth				Harvesting		
	Soybean			Sowing	Growth				Harvesting	

Figure 7. Crop calendars of corn and cotton in the Harran Plain and Corn, Cotton,Soybean in the Bismil Plain; and corn and soybean in Kansas.

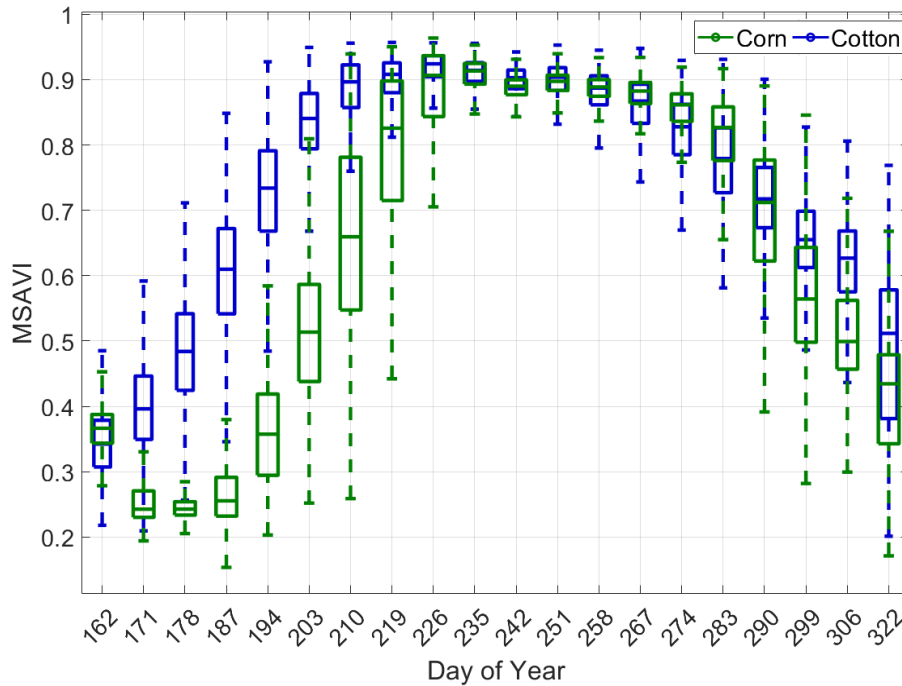


Figure 8. Box plots at each image acquisition in 2013 show variations in vegetation phenologies of all corn and cotton samples for the Harran dataset. Central mark indicates the median values. Bottom and top edges show 25th and 75th percentiles, respectively.

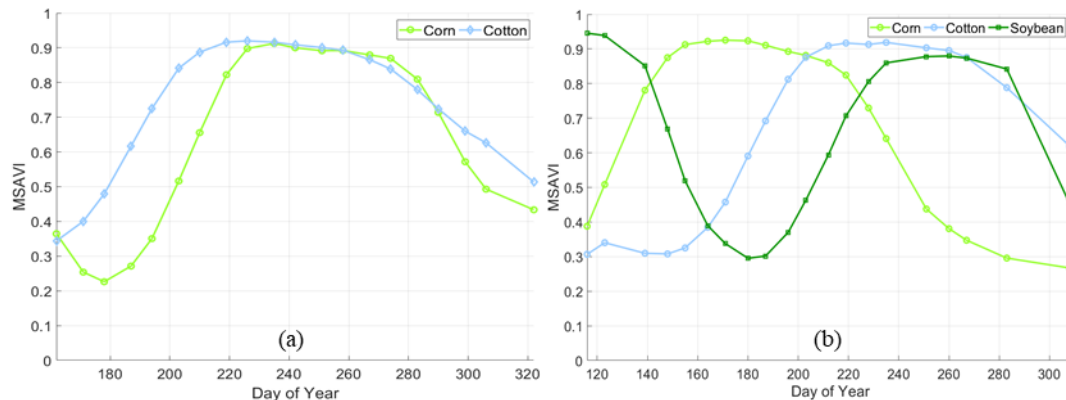


Figure 9. Median MSAVI phenologies of corn and cotton in the Harran Plain in 2013(a) and corn, cotton and soybean in the Bismil Plain in 2013(b).

3.2 Multi-year Crop Mapping Approach

An approach having high cross-year classification accuracy will benefit multi-year crop mapping studies. However, selecting training samples for each distinct location and crop at each year is difficult. In this study, a scheme is developed to classify crops with data from cross-years: training data are selected from one year while tests are performed with another year's data.

The proposed approach aims to present an efficient multi-year classification methodology as we incorporate cloud information cloning and time-series data smoothing.

A summary of the algorithm steps is presented in Figure 10. The vegetation index is computed from radiometrically corrected time-series satellite images. Atmospheric or illumination effects may degrade the performance of times series classification methods. Data smoothing methods have been used to reduce these effects [35], and in our work, we smoothed our (time-series) data by the Savitzky-Golay (SG) filtering method[36].

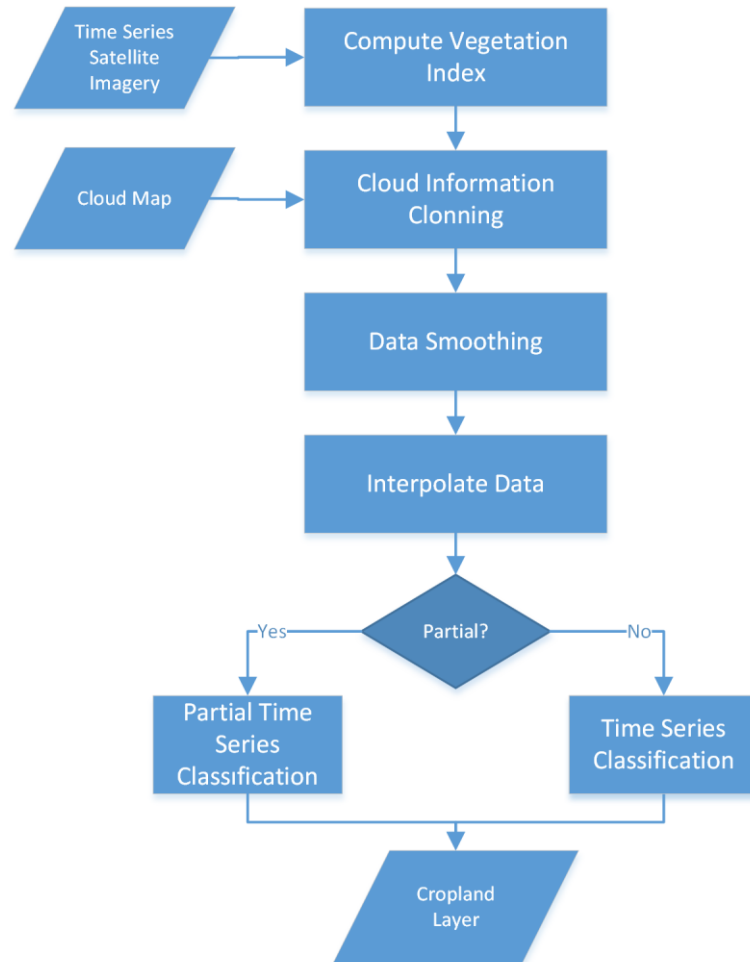


Figure 10. Multi-year Time-series Classification Algorithm Steps

Landsat 8 cloud and shadow masks are produced by the Fmask algorithm [37]. We applied cloud information cloning: cloudy samples were linearly interpolated with the Inverse Distance Weighting (IDW) method by using the nearest two cloud-free images [38]. Even though the Fmask algorithm could detect clouds successfully, it may not detect cloud shadows as effectively (Figure 11). However, we found the Fmask algorithm and SG smoothing, followed by median of time-series field phenology was adequate for successful classification. Kansas dataset uses the Harmonized Landsat 8 and Sentinel-2 satellite imagery (HLS). However, the Fmask algorithm (Fmask v3) which were used in HLS data is not optimal with Sentinel-2 data. This resulted in missed shadows and clouds in some cloudy Sentinel-2 scenes. Fmask. Moreover, we used Fmask version 4, which improved shadow and cloud detection with Sentinel-2 data. We used double sigmoid fitting instead of SG of crop phenologies to remove the remaining artifacts.

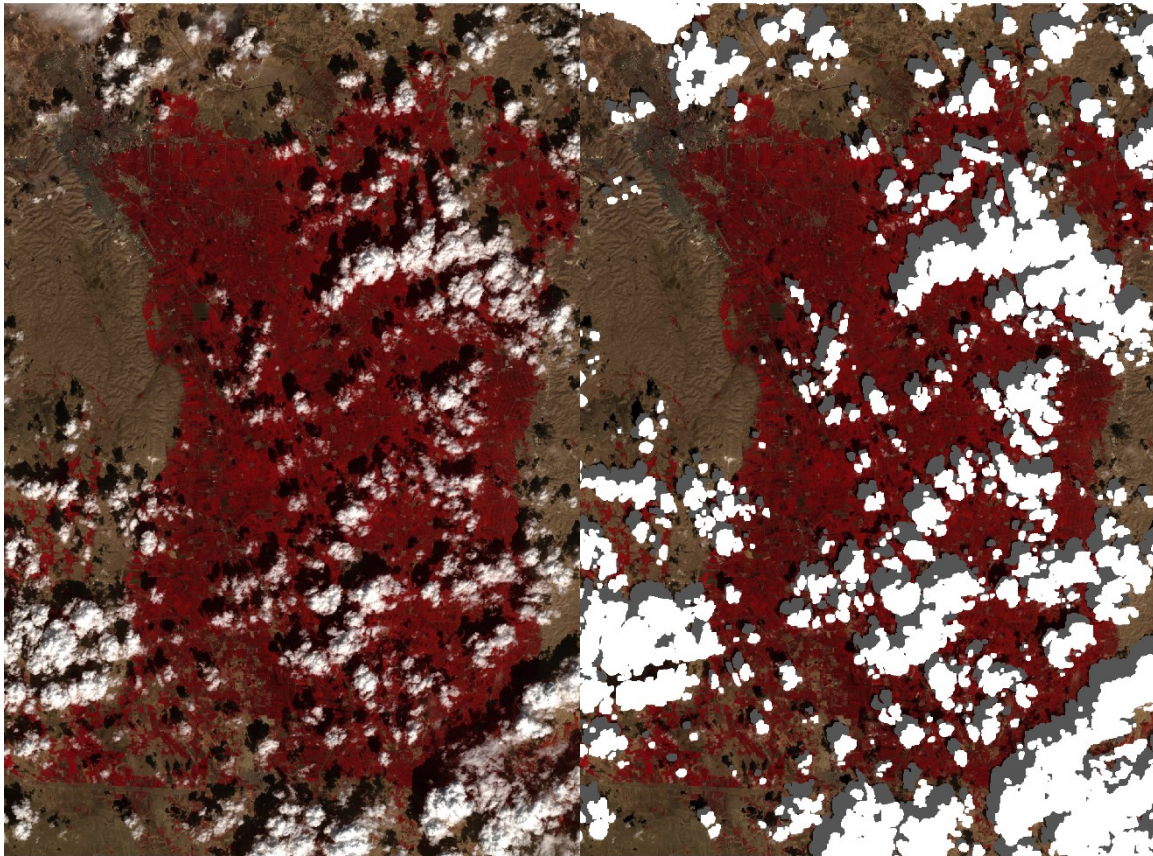


Figure 11 Clouds and their shadows detected by FMask algorithm.

To enable cross-year classification, data are linearly interpolated between $[t_l, t_u]$ where t_l and t_u are the lower and upper limits of the time-window. Time-series classification is used to classify with same-year or cross-year classification. Optionally, data is classified with a partial time-series approach. Finally, a cropland layer is produced showing the classification results.

3.3 Vector Dynamic Time Warping: VDTW

We studied phenological variations of a crop in various experimental settings within our datasets. For this purpose, we simulated crop signatures to analyze the behavior of DTW and spectral angle mapper (SAM) methods. Spectral angle mapper is a commonly used measure in hyperspectral image analysis describing the angular distance between two spectra [39]. Dynamic Time Warping (DTW) is a technique that finds the optimal alignment in translation and scaling between two time-series data sequences [40]. The sequences are matched in by dynamic programming to find optimal distances between signals. Shift and scale are simulated in different scenarios. These scenarios are given in the Appendix The scenarios aim to simulate farmers' practices, illumination, and climate changes both in the same-year and cross-years.

Our analyses with the simulations showed that both DTW and SAM have disadvantages while dealing with time-series phenological data since phenological measurements of crops at different dates may vary, as the weather and illumination conditions are not static.

We propose a new method, which is both robust to shift in crop growth and illumination differences: Vector Dynamic Time Warping (VDTW). While DTW is based on Euclidean distance d , we propose to use angular distance a as shown in Figure 12. VDTW computes the optimal warping path of spectral distances between two phenological observations. The length of the DTW search window should take into account the possible phenological variation between years. According to our experiments with various window sizes, the search window size was set to ± 15 days.

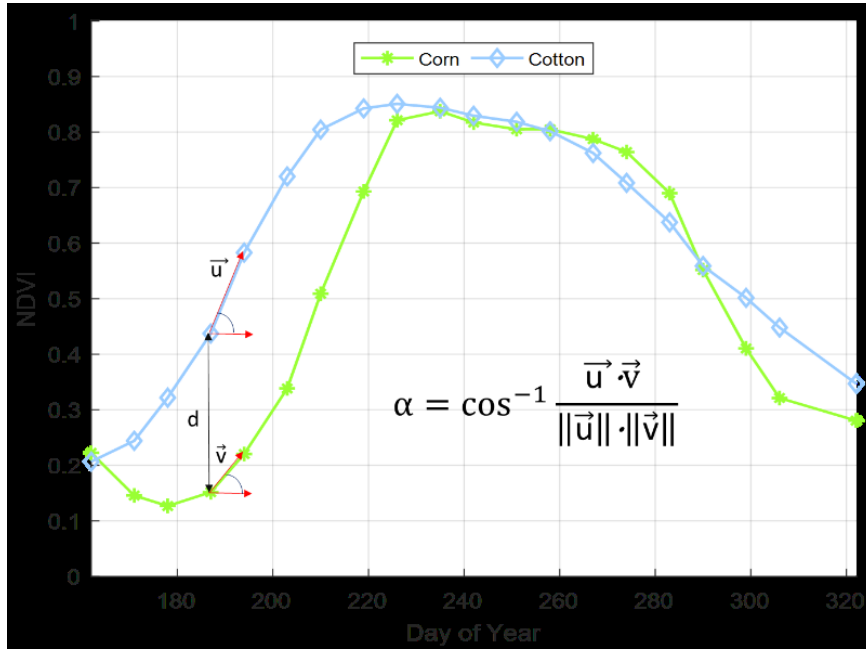


Figure 12. Angular distance metric between phenology of two crops at an observation date

The first step in VDTW algorithm is constructing n -by- m distance matrix Ψ whose elements $\psi_{i,j}$ is computed as the angle α between $\vec{u}_i \in U \forall i = 2, \dots, n$ and $\vec{v}_j \in V \forall j = 2, \dots, m$. \vec{u}_i and \vec{v}_j are unit vectors at each element. $\psi_{i,j}$ is computed as follow:

$$\psi_{i-1,j-1} = \cos^{-1} \frac{\vec{u}_i \cdot \vec{v}_j}{\|\vec{u}_i\| \cdot \|\vec{v}_j\|} \quad (1)$$

The accumulated $(m-1) \times (n-1)$ distance matrix, D , is computed from ψ by calculating the recursive sum of distances:

$$d_{i,j} = \psi_{i,j} + \min \{d_{i-1,j-1}, d_{i-1,j}, d_{i,j-1}\} \quad (2)$$

Computation is subject to following boundary conditions:

$$d_{i,j} = \begin{cases} \psi_{i,j} & i = 1, j = 1 \\ \sum_{k=2}^i \psi_{k,j} & 2 < i \leq n-1, j = 1 \\ \sum_{k=2}^j \psi_{i,k} & i = 1, 2 < j \leq m-1 \end{cases} \quad (3)$$

The source code of the VDTW method is available at GitHub: <https://github.com/mustafateke/VDTW>

3.4 Partial Time-Series Classification

A new method is presented in the previous section. In this study, we also propose a partial time-series approach which achieves high classification accuracies with fewer data acquisitions, using distinct time-periods of crop phenologies.

For example, corn and cotton in the Harran Plain are sown at a specific date; however, they both start to have the same phenological properties beginning from mid-August, after which their growths are nearly the same. Corn and cotton can be discriminated in their early growth until mid-August (Figure 8). Our method exploits this phenologically invariant region for improved cross-year crop classification.

The partial time-series algorithm has three significant steps. The algorithm finds the optimal classification window around the pivot day.

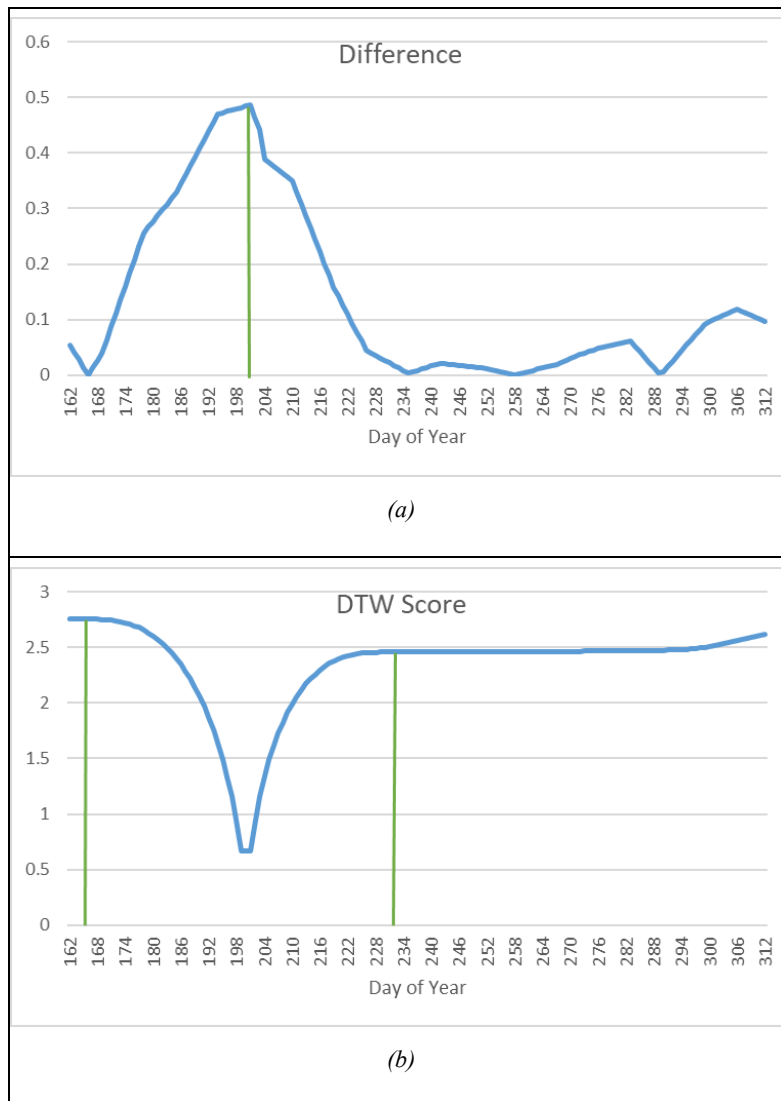
Algorithm steps:

First, the pivot day where the difference between the vegetation index (VI) of crops is maximum is determined (Figure 13(a)). Median values of all samples from each crop are used in this computation. The pivot day is determined as:

$$J^* = \arg \max_{t_l < J < t_u} \text{abs}(VI_{C_1}(J) - VI_{C_2}(J)) \quad (4)$$

where J^* denotes pivot day, C_1 and C_2 are

first and second crops, t_l denotes the minimum common day and, t_u denote the maximum common day shared by time-series data of all years.



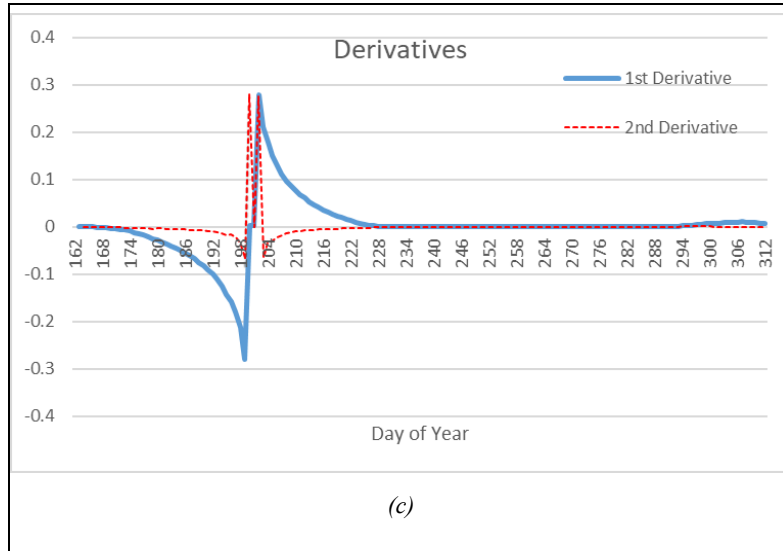


Figure 13. (a) The maximum difference of VI values between corn and cotton, (b) DTW scores between corn and cotton centered on the pivot day expanding on both sides, (c) First and second derivatives of DTW scores.

DTW scores of vectors extending in both directions are computed by centering the pivot day (Figure 13(b)). Lower DTW scores correspond to higher similarity. The increase in DTW scores is steady after specific periods, which coincides with discriminative regions of corn and cotton.

$$Score(J) = DTW(VI_1([J^*, J]), VI_2([J^*, J])) \quad (5)$$

where $t_l < J < t_u$.

We find the first days from the pivot by extending to initial and final dates until first and second derivatives are zero (Figure 13(c)). First and second derivatives indicate that DTW scores are steady after these days, as a result determining the boundaries of the optimal time window.

$$find\ score(J)' = 0\ AND\ score(J)'' = 0 \quad (6)$$

The optimal time window $[o1, o2]$ for classification of corn and cotton are computed as day 170 and day 227, corresponding to mid-June and mid-August. In the case of three or more crops, each crop is compared to others and the minimum length time window is selected against other crops.

4. Results

In our study, we used median of each field as a sample. Median of a field is computed from the center region of it after its boundaries is buffered by 50 meters to reduce boundary effects. We also increase reliability of our tests by eliminating registration errors between multi-temporal scenes and misalignment between fields vectors and satellite imagery by applying a buffer. A stratified random selection strategy was applied to training sample selection [41], and selected training samples were excluded from the test samples in same-year tests. The same training samples for each test are used in training for all methods. Tests were repeated 100 times to minimize the effect of non-representative outlier samples such as crops grown too early or too late. We compared different methods against various numbers of training samples to evaluate their performance with a limited number of training samples. Congalton suggested using at least 50 samples from each class when the number of classes is less than 12 [42]. We varied the number of training samples in 5, 10, ..., 50 based on their findings.

Detailed tests are performed for same-year and cross-year classification accuracies. Double sigmoid features with RF classifier and SVM, Time-series (VDTW, SAM, and DTW, TWDTW) and partial time-series (PVDTW) were compared in this study. RF classifier contains 1000 trees. SVM has

the RBF kernel, and its parameters are selected after an extensive grid search of cross-validation of training samples. As DL methods gained much attention in classification, we used two-layer deep long short-term memory (LSTM) with 100 units at each layer followed by a softmax layer [43].

In our cross-year tests, the Harran dataset is the most challenging since corn and cotton's phenologies vary each year after peak growth until the harvest. Same-year and cross-year percent overall accuracy scores of tested methods are shown in Table 4. Our tests have shown that VDTW provides the highest overall accuracies both in the same year at 99.83% (Figure 14) and cross-year at 99.40% (Figure 15).

SAM and RF methods had similar accuracies in the same year; however, RF was not robust to growth changes in the cross-year as SAM. SAM cross-year scores were below 96.53%. RF was only able to reach 94.45% with a maximum number of training samples. VDTW was more robust to shifts in growth and changes in illumination compared to other methods. The best two performers VDTW and TWDTW achieved the cross-year 50 training sample and 100-replication overall average classification accuracies of 99.40% and 96.66%, respectively. The 95% confidence interval for overall accuracy differences between VDTW and TWDTW methods were between 2.63% and 2.86%. Since 0 is not in the included in the 95% confidence interval, our results support that the algorithms are significantly different from each other for the Harran dataset. (Table 4). TWDTW's time cost improved DTW's cross-year overall accuracy from 94.97% to 96.66%. Time series with Deep LSTM initially produced lower accuracies for training sample size < 20 for each class. Deep LSTM obtained similar overall accuracies with DTW and SAM for the training sample size of 50 (~1 of samples) for each class. We increased deep LSTM training sample size to 80/20 ratio of training and test data to obtain overall accuracies average 99.75% for the same year and 98.34% for the cross-year.

Tests with a varying number of training samples reveal that VDTW maintained high classification accuracies with a fewer number of samples compared to other methods as shown in Figure 14-Figure 17. In other words, the advantage of the proposed approach is its ability to attain high classification accuracy independent of the training set size.

Partial time-series applied to VDTW also achieved similar accuracy values as the core method. Partial time-series the applied version of VDTW, PVDTW, reduces the amount of data by using fewer data limited by time windows. These time windows are based on phenological differences between crops.

In the Bismil dataset, VDTW, TWDTW, and SAM obtained highest overall accuracies both in the same-year and cross-year regardless of the training set size while TWDTW was marginally better (Figure 16 & Figure 17). The 95% confidence interval for overall accuracy differences between TWDTW and VDTW were between 0.0085% and 0.0349%. Since 0 is not in the included in the 95% confidence interval, our results support that the algorithms are significantly different from each other for the Bismil dataset. The same-year and cross-year percent overall accuracy scores of tested methods are shown in Table 5.

RF and SVM classifiers, which use features extracted from time-series data, have lower performance than other methods in the tests. Performances of RF and SVM are lower since curve fitting is designed for single cropping and may not always fit the optimal curve for double cropping case. Time-series methods such as proposed VDTW, SAM, and DTW are robust to double cropping cases.

Finally, we tested VDTW method with data from Kansas. Crops in Kansas are distinctly grown. Same year crop mapping accuracies were high for all classifiers as shown in Table 6. TWDTW method obtained highest the same-year overall accuracy of 99.02% followed by VDTW and LSTM having overall accuracies of 98.74% and 98.60%. On the other hand, VDTW resulted higher overall accuracies than TWDTW by 1.72% and other methods in the cross-year tests.

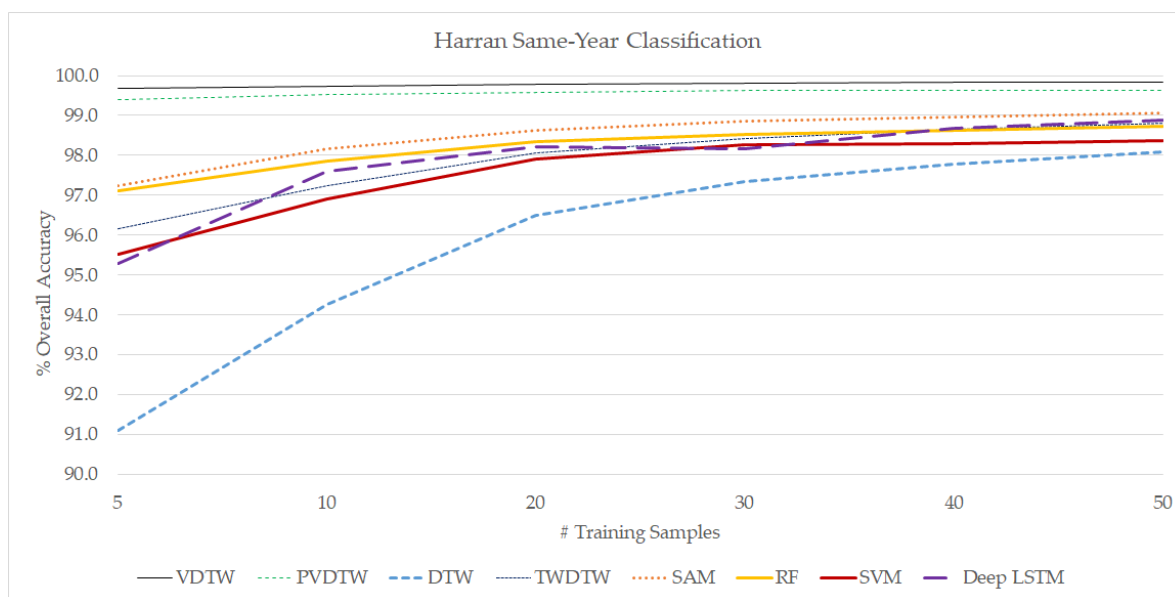


Figure 14. Harran dataset same-year classification results at various training sample sizes.

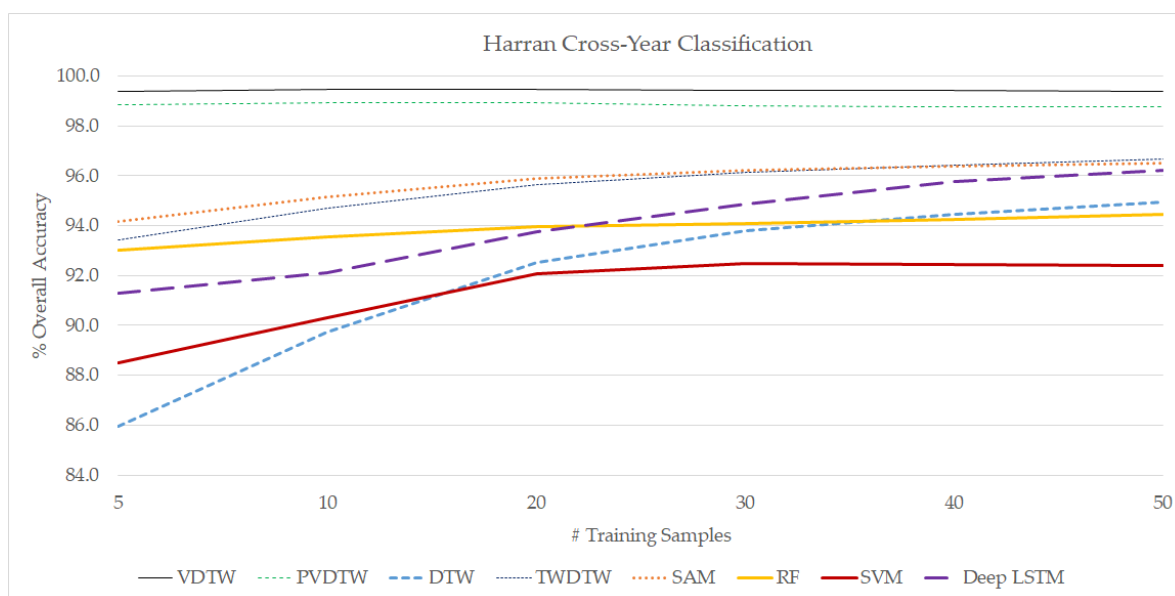


Figure 15. Harran dataset same-year classification results at different training sample sizes.

Table 4. Percent average overall accuracies of proposed and compared methods with 50 samples from each class for the Harran Dataset. Samples are selected with the stratified random selection

	VDTW	PVDTW	DTW	TWDTW	SAM	RF	SVM	Deep LSTM
Same-year	99.83	99.63	98.08	98.81	99.05	98.72	98.36	98.87
Cross-year	99.40	98.75	94.97	96.66	96.53	94.45	92.40	96.21

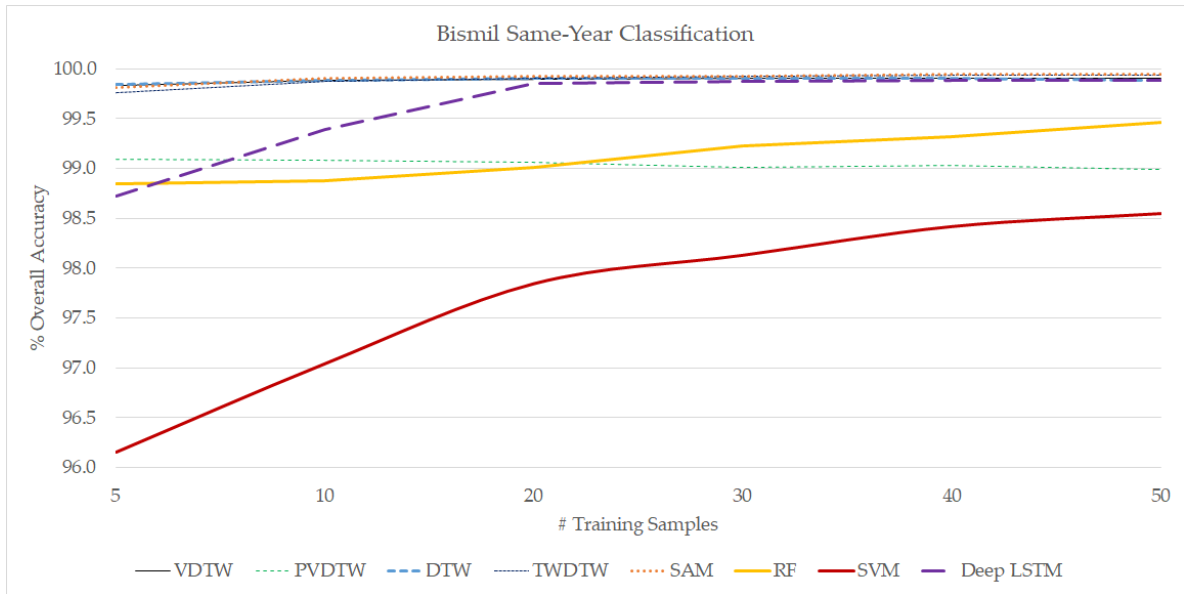


Figure 16. Bismil dataset same-year classification results at various training sample sizes.

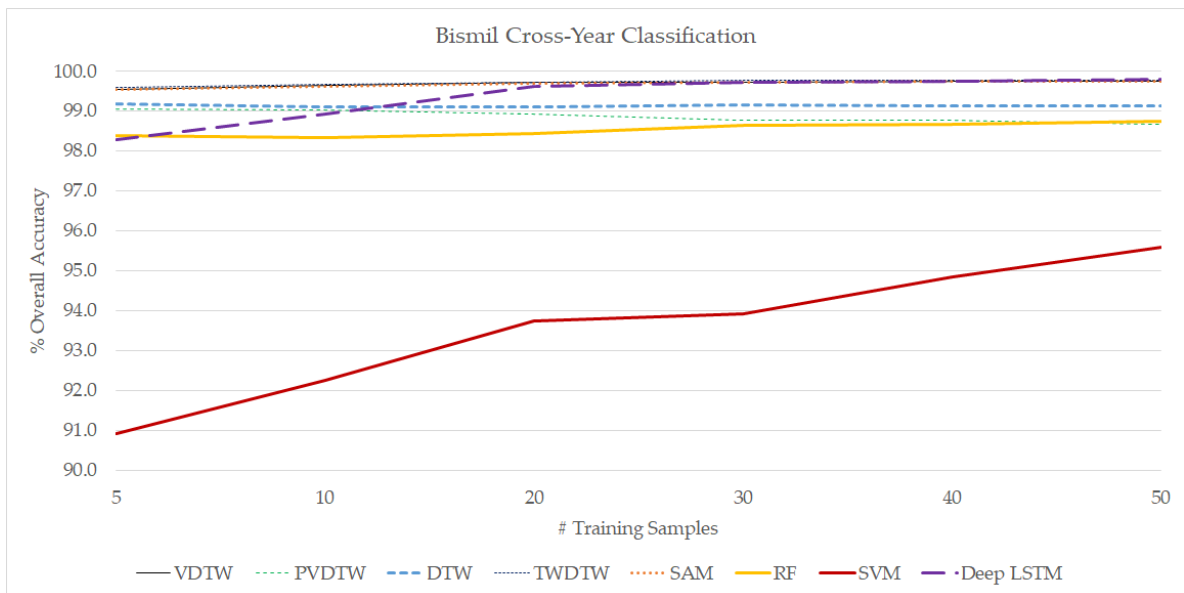


Figure 17. Bismil dataset cross-year classification results at different training sample sizes.

Table 5. Percent average overall accuracies of proposed and compared methods with 50 samples from each class for the Bismil Dataset. Samples are selected with the stratified random selection

	VDTW	PVDTW	DTW	TWDTW	SAM	RF	SVM	Deep LSTM
Same-year	99.90	98.99	99.89	99.94	99.94	99.46	98.55	99.88
Cross-year	99.74	98.67	99.13	99.78	99.76	98.75	95.60	99.80

Table 6. Percent average overall accuracies of proposed and compared methods with 50 samples from each class for the Kansas Dataset. Samples are selected with the stratified random selection

	VDTW	PVDTW	DTW	TWDTW	SAM	RF	SVM	Deep LSTM
Same-year	<u>98.74</u>	97.47	80.81	99.02	98.72	98.31	97.87	98.60
Cross-year	<u>90.12</u>	85.10	75.35	88.40	86.06	85.67	86.23	87.48

User's accuracy and producer's accuracy for the Harran dataset are presented in Table 7. User's accuracies are similar for both crops; however, several mislabeled corns result in lower producer's accuracy for corn. Both user's and producer's accuracies of cotton are over 99% in same-year tests and 98% in cross-year tests.

Table 7. Average User's Accuracy and Producer's Accuracy of VDTW classification results with 50 samples for the same-year and cross-year.

	User's Accuracy		Producer's Accuracy	
	Corn	Cotton	Corn	Cotton
Same-year	99.44	99.89	99.21	99.92
Cross-year	98.05	99.79	98.24	99.53

High user's accuracy both in the same and cross-year tests show that misclassification percentage of corn and cotton is low. However, low user's accuracy of corn indicates that 1.95% of corn is labeled as cotton in cross-year tests. Misclassification error is 0.46% in the same-year tests. Kappa values were 1.00 for the same-year tests and 0.99 for the cross-year tests.

A detailed view of VDTW classification is provided in the form of confusion tables. Confusion matrix in Table 8 shows the number of fields which were correctly classified as corn and cotton with training data from the same or other years. Cotton was correctly classified while some percent of corn is misclassified as cotton.

Table 8. Average Confusion Matrix of 100 tests for VDTW Classification with 50 samples in the Harran Plain. Columns are observations while rows are predictions. Years in rows are training and years in rows are test years.

		2013		2014		2015		2016	
		Corn	Cotton	Corn	Cotton	Corn	Cotton	Corn	Cotton
2013	Corn	1109	3	716	1	821	6	379	0
	Cotton	8	4030	6	4600	3	3429	13	3745
2014	Corn	1155	42	668	1	823	16	380	0
	Cotton	12	4041	4	4550	1	3419	12	3745
2015	Corn	1141	9	716	1	773	5	379	0
	Cotton	26	4074	7	4600	1	3380	13	3745
2016	Corn	1160	124	720	17	823	35	338	4
	Cotton	7	3959	2	4584	1	3400	4	3691

Classification accuracy of cotton was above 99.81% in the same-year tests and 99.64% in cross-year tests. The accuracy of corn was as low as 91.81% in cross-year tests in 2016. The difference in classification accuracies was partly due to how corn is sown after the harvest of wheat, so a late harvest of wheat may shift the growth of corn in different years. On the other hand, the plantation of cotton is not dependent on other agricultural activities.

As the distinct growth times of crops in the Bismil dataset allow classifiers to reach high classification results, VDTW has high same and cross-year accuracies.

Both user's and producer's accuracies are close to 100% (Table 9). Cross-year producer's accuracy of cotton shows that 1% of cotton classified incorrectly and labeled as corn. Kappa values were 0.99 for the same-year and the cross-year tests.

Table 9. Average User's Accuracy and Producer's Accuracy of VDTW classification results with 50 samples in the Bismil Plain for the same-year and cross-year.

	User's Accuracy			Producer's Accuracy		
	Corn	Cotton	Soybean	Corn	Cotton	Soybean
Same-year	99.87	99.96	100	99.98	99.70	100
Cross-year	99.57	99.98	99.99	99.99	99.06	100

Confusion matrix of the Kansas dataset is depicted in **Error! Not a valid bookmark self-reference..** The same year user's and producer's accuracies of corn and soybean are above 98%. However cross year accuracies are lower (Table 6, Table 10, Table 11). VDTW mislabel 22.84% of corn fields trained with 2018 data and tested with 2017 and 13.98% of soybean fields trained with 2018 data and tested with 2017 data. Crops in 2018 were sown eight days earlier on average compared to 2017. This caused lower accuracies in the cross-year tests.

Table 10. Average Confusion Matrix of 100 tests for VDTW Classification with 50 samples in the Kansas dataset. Columns are observations while rows are predictions. Years in rows are training and years in rows are test years.

		2017		2018	
		Corn	Soybean	Corn	Soybean
2017	Corn	2048	142	2283	429
	Soybean	78	2855	24	2630
2018	Corn	1679	31	2224	76
	Soybean	497	3016	33	2933

Table 11. Average User's Accuracy and Producer's Accuracy of VDTW classification results with 50 samples for the same-year and cross-year for the Kansas Dataset.

	User's Accuracy		Producer's Accuracy	
	Corn	Soybean	Corn	Soybean
Same-year	98.33	99.04	98.67	98.79
Cross-year	91.17	92.48	88.06	92.47

Same year user's and producer's accuracies are between 98.33-99.04% (Table 11). However, the cross-year user's and producer's accuracies are up to 10% lower. Kappa values were 0.97 for the same-year and 0.81 for the cross-year tests.

4. Discussion

Test results show that the proposed approach improved overall accuracy results in both the same-year and cross-year tests. VDTW fuses advantages of both DTW and SAM methods thus it provides flexibility in time and measurement variations: DTW has the ability to be flexible in time; SAM is robust to illumination changes and measurement differences.

Previous work had an overall accuracy difference of 10% between same-year and cross-year [18]. The proposed approach also improved same-year crop mapping accuracies in the Harran Plain compared to previous object-based [44] and multi-temporal [45] studies. Our results with the Kansas dataset was also in conjunction of the previous work[18] having 9% to 10% accuracy difference

between the same-year and the cross-year tests. Yearly change of cropping practices decreased accuracy of all classification methods in the Kansas dataset. On the other hand, VDTW method was more robust compared to other methods in the cross-year tests. TWDTW approach was proposed to improve DTW performance [46]. However, it did not include changes in illumination and variations in measurements as in SAM or VDTW approach. Deep LSTM's accuracy was improved as the number of training samples were increased. This result was expected as DL requires a large amount of data and fine-tuning of parameters. RF with a double-sigmoid features approach has similar results compared to SAM and DTW methods. However performance values were lower in the double cropping case of the Bismil dataset. Double-sigmoid feature extraction should be improved for multiple cropping cases.

Our multiyear crop mapping approach overcame difficulties in cross-year classification. In addition to SG data smoothing, we included interpolation of vegetation index values of cloudy data samples. This cloud information cloning approach improved cross-year overall accuracies.

NDVI and EVI were commonly used in phenological feature extraction [47,48]. However, We propose the use of MSAVI Since we obtained higher the cross-year overall accuracies with the use of the MSAVI. Soil adjusted vegetation indices, such as SAVI, include the effect of the soil line as a parameter; on the other hand, MSAVI computes the soil line parameter automatically. For this reason, the use of MSAVI further reduced variations in observation angles.

A limited time window version of VDTW, PVDTW, achieved similar overall accuracies with fewer data. PVDTW enables mid-season crop classification and has efficient computation requirements. The partial window method may be applied to other classification algorithms such as DTW and SAM under the proposed multi-year crop mapping approach.

VDTW and PVDTW methods are not as vulnerable as the other methods to the paucity of available training data. This property is useful since an operational system can use pure phenologies (as low as a single time-series signature) or it can still operate sufficiently with fewer temporal data samples.

The proposed methods can also be extended to the classification of other crops, such as discrimination of wheat-barley, corn-soybean [21], and rice-corn [49], which have overlapped phenological phases.

The difference of the first derivative of vegetation index (VI) was evaluated as an alternative to angles between VI time-vectors. The correlation between two distinct vectors, which have different values and the same slopes, were different. VDTW incorporates Euclidean similarity implicitly thus resulting in better discrimination.

We consider missing data acquisitions in large time windows may lower multi-year crop mapping performances. These time windows are growth and harvest where the changes are exponential rather than linear. We suggest that the curve fitting with the double logistic function or other non-linear methods may eliminate this problem.

According to our investigations in the Harran Plain, farmers may re-sow cotton if the seedlings did not emerge due to drought or heavy rains. In this case, the growth of the cotton crop was delayed and its phenology resembled that of corn. Another issue is the growing of cotton as the second crop. However, this practice is not common and may produce low crop yields [50].

One last challenge for VDTW method is that it requires more computation power than both DTW and SAM methods. Compared to the DTW, vector dot products is computed at each point instead of a simple absolute distance operation. However, VDTW achieved high performance with fewer training samples. We also suggest using the median of training samples to generate crop mapping from training data for time-sensitive or large-scale applications.

5. Conclusions

In this study, vector dynamic time warping (VDTW), an improved version of DTW, was developed and presented in a multi-year crop mapping approach for efficiently classifying crops with similar phenologies, such as corn and cotton, and other crops with distinct phenologies. The proposed method is based on optimal time vector alignment of crop phenologies for overcoming the

difficulties experienced in previous efforts. Vector dynamic time warping (VDTW) for crop mapping is robust against spectral and temporal shifts in yearly crop growths.

We tested our method with multiple crops and in separate regions yielding high classification accuracies. Classification of corn and cotton, which are investigated in this study is challenging due to the overlaps in their phenological characteristics. On the other hand, the crops in the Bismil Plain have distinct phenologies. Corn and Soybean in Kansas have partially overlapping phenologies however phenology of crops in 2018 shifted considerably compared to 2017. The proposed VDTW method provided the highest same-year and cross-year overall classification accuracies. Our tests with the Kansas dataset showed that there are still room for improvement in cross-year crop mapping.

Another improvement of our work is employing discriminative regions for efficient crop classification PVDTW method uses optimal time window selection to achieve comparable accuracies of its base method, with less temporal data. Optimal time-periods to discriminate these crops are determined by our algorithm.

Both VDTW and PVDTW methods achieved higher classification accuracy compared to other methods with a limited number of training samples, thus reducing the repeated effort of collecting ground samples.

We believe that the proposed methods can also be expanded to classify other types of crops. Besides, the VDTW method may also be adapted to different research areas (e.g., data mining and speech recognition) where DTW is commonly preferred.

We also believe that the approach developed is highly suitable for crop mapping at nationwide scales. However, further additional datasets are required to expand the VDTW to countrywide levels. In the meantime, we think that the proposed approach may be used to improve the accuracy of the Ministry of Agriculture and Forestry's National Registry of Farmers in the near future for the crop types taken into consideration in this study.

Appendix A

Figure A1(a) shows the case if sowing dates vary while harvest dates are the same. Figure A1(b) shows crops are sown at the same time but harvest dates differ. In Figure A1(c), an extreme case is shown, where the crop's both sow and harvest times vary. Figure A1(d) shows where growth duration of the crop stays same, but its sow and harvest time shifts in time: this simulation corresponds to some growers sowing earlier or later and yearly climate changes. Figure A1(e) depicts variances in phenological observation in the growing period. These differences may be caused by different atmospheric conditions or variations in fields or farming practices. Finally, an extreme case is displayed in Figure A1(f). Note that these graphs may be applied to any vegetation index. For the sake of simplicity NDVI was chosen.

The DTW method was able to obtain the minimum distance between signals where time varies (Figure A1(a-d)). On the other hand, SAM method scores were below 0.2 radians for the cases shown in Figure A1(e-f). VDTW was able to obtain the lowest scores in all cases.

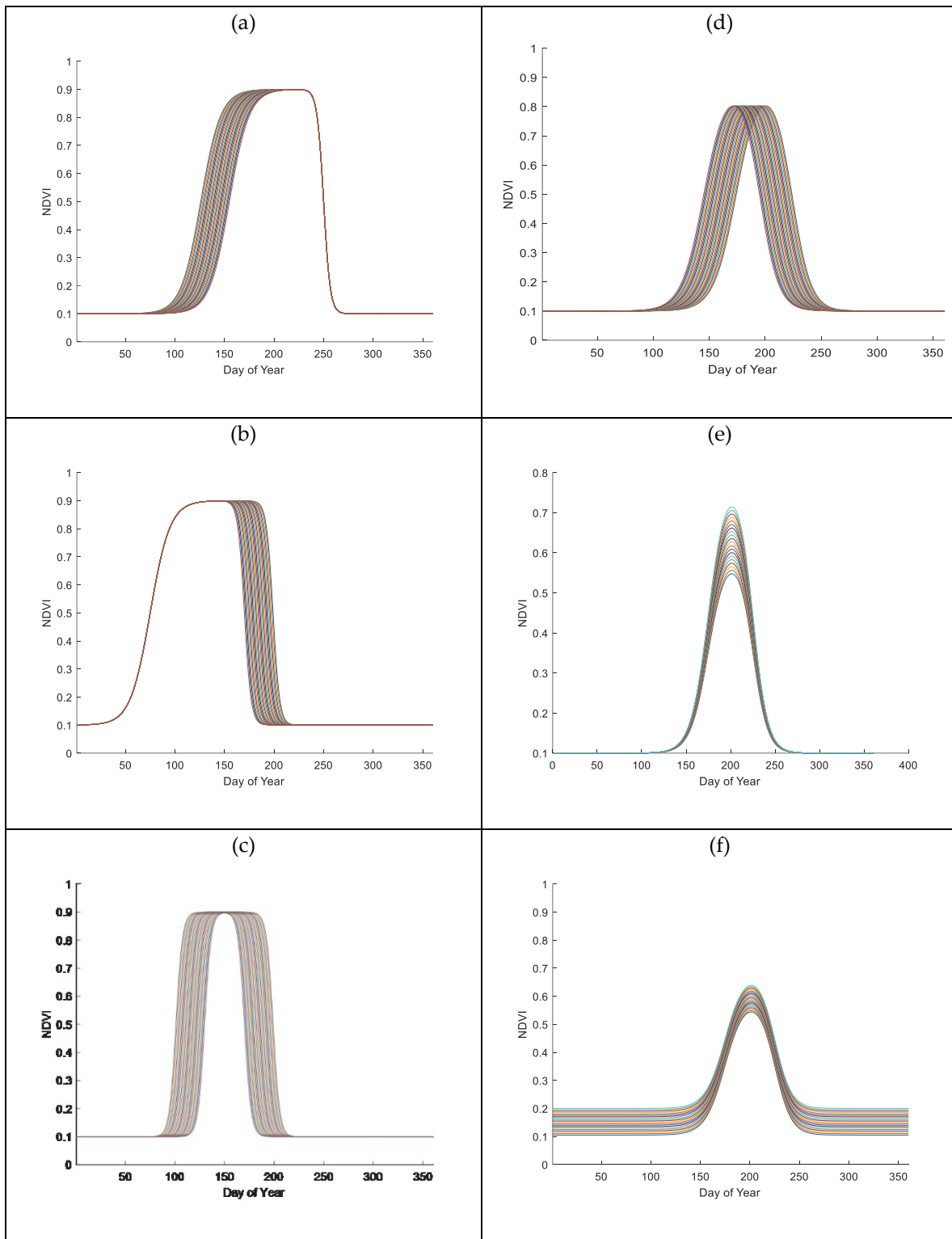


Figure A1. Various simulations of virtual crops: (a) sown at earlier dates harvested at the same time, (b) sown at the same time, harvested later, (c) variations both in sow and harvest dates, (d) crop sowing and harvest dates shift in time, (e) crops are grown in the same time period with various amount of health/nutrition, (f) extreme case of bias in NDVI values up to 0.1.

References

1. United Nations *World Population Prospects: The 2015 Revision, Key Findings and Advance Tables*. Working Paper No. ESA/P/WP.241; 2015;
2. Rembold, F.; Maselli, F. Estimation of inter-annual crop area variation by the application of spectral angle mapping to low resolution multitemporal NDVI images. *Photogramm. Eng. Remote Sens.* **2006**, *72*, 55–62.
3. Jansen, L.J.M.; Badea, A.; Milenov, P.; Moise, C. Land Use and Land Cover Mapping in Europe. **2014**, *18*.
4. Esetlili, M.T.; Bektas Balcik, F.; Balik Sanli, F.; Ustuner, M.; Kalkan, K.; Goksel, C.; Gazioğlu, C.; Kurucu, Y. Comparison of Object and Pixel-Based Classifications For Mapping Crops Using Rapideye Imagery: A Case Study Of Menemen Plain, Turkey. *Int. J. Environ. Geoinformatics* **2018**, *5*, 231–243.
5. Şimşek, Fatih Fehmi ;Teke, Mustafa;Altuntaş, C. Controlling of Product Declarations of Farmers Using Remote Sensing Techniques: The Harran Plain Case. In Proceedings of the 6. Uzaktan Algılama ve CBS Sempozyumu - UZAL-CBS 2016; 2016; pp. 276–286.
6. Gómez, C.; White, J.C.; Wulder, M.A. Optical remotely sensed time series data for land cover classification: A review. *ISPRS J. Photogramm. Remote Sens.* **2016**, *116*, 55–72.
7. Congalton, R.; Gu, J.; Yadav, K.; Thenkabail, P.; Ozdogan, M.; Congalton, R.G.; Gu, J.; Yadav, K.; Thenkabail, P.; Ozdogan, M. Global Land Cover Mapping: A Review and Uncertainty Analysis. *Remote Sens.* **2014**, *6*, 12070–12093.
8. García-Mora, T.J.; Mas, J.-F.; Hinkley, E.A. Land cover mapping applications with MODIS: a literature review. *Int. J. Digit. Earth* **2012**, *5*, 63–87.
9. Ok, A.O.; Akyurek, Z. A segment-based approach to classify agricultural lands by using multi-temporal optical and microwave data. *Int. J. Remote Sens.* **2012**, *33*, 7184–7204.
10. Ozdarici-Ok, A.; Akyurek, Z. OBJECT-BASED CLASSIFICATION OF MULTI-TEMPORAL IMAGES FOR AGRICULTURAL CROP MAPPING IN KARACABEY PLAIN, TURKEY. *ISPRS-International Arch. Photogramm. Remote Sens. Spat. Inf. Sci.* **2014**, *1*, 127–132.
11. Long, J.A.; Lawrence, R.L.; Greenwood, M.C.; Marshall, L.; Miller, P.R. Object-oriented crop classification using multitemporal ETM+ SLC-off imagery and random forest. *GIScience Remote Sens.* **2013**, *50*, 418–436.
12. Löw, F.; Conrad, C.; Michel, U. Decision fusion and non-parametric classifiers for land use mapping using multi-temporal RapidEye data. *ISPRS J. Photogramm. Remote Sens.* **2015**, *108*, 191–204.
13. Liu, J.; Feng, Q.; Gong, J.; Zhou, J.; Liang, J.; Li, Y. Winter wheat mapping using a random forest classifier combined with multi-temporal and multi-sensor data. *Int. J. Digit. Earth* **2018**, *11*, 783–802.
14. Petitjean, F.; Weber, J. Efficient Satellite Image Time Series Analysis Under Time Warping. *Geosci. Remote Sens. Lett. IEEE* **2014**, *11*, 1143–1147.
15. Tatsumi, K.; Yamashiki, Y.; Torres, M.A.C.; Taibe, C.L.R. Crop classification of upland fields using Random forest of time-series Landsat 7 ETM+ data. *Comput. Electron. Agric.* **2015**, *115*, 171–179.
16. Zheng, B.; Myint, S.W.; Thenkabail, P.S.; Aggarwal, R.M. A support vector machine to identify irrigated crop types using time-series Landsat NDVI data. *Int. J. Appl. Earth Obs. Geoinf.* **2015**, *34*, 103–112.
17. Shao, Y.; Lunetta, R.S. Comparison of support vector machine, neural network, and {CART} algorithms for the land-cover classification using limited training data points. *ISPRS J. Photogramm. Remote Sens.* **2012**, *70*, 78–87.
18. Zhong, L.; Gong, P.; Biging, G.S. Efficient corn and soybean mapping with temporal extendability: A multi-year experiment using Landsat imagery. *Remote Sens. Environ.* **2014**, *140*, 1–13.

19. Maus, V.; Câmara, G.; Cartaxo, R.; Sanchez, A.; Ramos, F.M.; de Queiroz, G.R. A time-weighted dynamic time warping method for land-use and land-cover mapping. *IEEE J. Sel. Top. Appl. Earth Obs. Remote Sens.* **2016**, *9*, 3729–3739.
20. Belgiu, M.; Csillik, O. Sentinel-2 cropland mapping using pixel-based and object-based time-weighted dynamic time warping analysis. *Remote Sens. Environ.* **2018**, *204*, 509–523.
21. Massey, R.; Sankey, T.T.; Congalton, R.G.; Yadav, K.; Thenkabail, P.S.; Ozdogan, M.; Sánchez Meador, A.J. MODIS phenology-derived, multi-year distribution of conterminous U.S. crop types. *Remote Sens. Environ.* **2017**, *198*, 490–503.
22. Pringle, M.J.; Schmidt, M.; Tindall, D.R. Multi-decade, multi-sensor time-series modelling—based on geostatistical concepts—to predict broad groups of crops. *Remote Sens. Environ.* **2018**, *216*, 183–200.
23. Lecun, Y.; Bengio, Y.; Hinton, G. Deep learning. *Nature* **2015**, *521*, 436–444.
24. Kamilaris, A.; Prenafeta-Boldú, F.X. Deep learning in agriculture: A survey. *Comput. Electron. Agric.* **2018**, *147*, 70–90.
25. Liakos, K.; Busato, P.; Moshou, D.; Pearson, S.; Bochtis, D. Machine Learning in Agriculture: A Review. *Sensors* **2018**, *18*, 2674.
26. Kussul, N.; Lavreniuk, M.; Skakun, S.; Shelestov, A. Deep Learning Classification of Land Cover and Crop Types Using Remote Sensing Data. *IEEE Geosci. Remote Sens. Lett.* **2017**, *14*, 778–782.
27. Ozdogan, M.; Woodcock, C.E.; Salvucci, G.D.; Demir, H. Changes in summer irrigated crop area and water use in Southeastern Turkey from 1993 to 2002: Implications for current and future water resources. *Water Resour. Manag.* **2006**, *20*, 467–488.
28. Çelik, M.A.; Gülersoy, A.E. Güneydoğu Anadolu Projesi'nin (GAP) Harran Ovası Tarımsal Yapısında Meydana Getirdiği Değişimlerin Uzaktan Algılama ile İncelenmesi. *J. Int. Soc. Res.* **2013**, *6*.
29. *Landsat 8 Surface Reflectance Product Guide v1.2*; 2015;
30. Claverie, M.; Ju, J.; Masek, J.G.; Dungan, J.L.; Vermote, E.F.; Roger, J.-C.; Skakun, S. V.; Justice, C. The Harmonized Landsat and Sentinel-2 surface reflectance data set. *Remote Sens. Environ.* **2018**, *219*, 145–161.
31. Yomralioglu, T.; Inan, H.I.; Aydinoglu, A.C.; Uzun, B. *Scientific research and essays*; Academic Journals, 2009; Vol. 4.
32. Sun, P.; Congalton, R.G.; Pan, Y. Using a simulation analysis to evaluate the impact of crop mapping error on crop area estimation from stratified sampling. *Int. J. Digit. Earth* **2018**, 1–21.
33. Huete, A.R.; Hua, G.; Qi, J.; Chehbouni, A.; van Leeuwen, W.J.D. Normalization of multidirectional red and NIR reflectances with the SAVI. *Remote Sens. Environ.* **1992**, *41*, 143–154.
34. of Agriculture-National Agricultural Statistics Service, (USDA-NASS) U S Department Usual planting and harvesting dates for US field crops. 2010.
35. Arvor, D.; Jonathan, M.; Meirelles, M.S.P.; Dubreuil, V.; Lecerf, R. Comparison of Multitemporal MODIS-EVI Smoothing Algorithms and its Contribution to Crop Monitoring. In Proceedings of the Geoscience and Remote Sensing Symposium, 2008. IGARSS 2008. IEEE International; 2008; Vol. 2, pp. II-958-II-961.
36. Kim, S.-R.; Prasad, A.K.; El-Askary, H.; Lee, W.-K.; Kwak, D.-A.; Lee, S.-H.; Kafatos, M. Application of the Savitzky-Golay Filter to Land Cover Classification Using Temporal MODIS Vegetation Indices. *Photogramm. Eng. Remote Sens.* **2014**, *80*, 675–685.
37. Zhu, Z.; Woodcock, C.E. Object-based cloud and cloud shadow detection in Landsat imagery. *Remote Sens. Environ.* **2012**, *118*, 83–94.

38. Kalkan, K.; Maktav, M.D. A Cloud Removal Algorithm to Generate Cloud and Cloud Shadow Free Images Using Information Cloning. *J. Indian Soc. Remote Sens.* **2018**, *46*, 1255–1264.
39. Kruse, F.A.; Lefkoff, A.B.; Dietz, J.B. Expert system-based mineral mapping in northern death valley, California/Nevada, using the Airborne Visible/Infrared Imaging Spectrometer (AVIRIS). *Remote Sens. Environ.* **1993**, *44*, 309–336.
40. Müller, M. Dynamic time warping. *Inf. Retr. Music motion* **2007**, 69–84.
41. Olofsson, P.; Foody, G.M.; Herold, M.; Stehman, S. V; Woodcock, C.E.; Wulder, M.A. Good practices for estimating area and assessing accuracy of land change. *Remote Sens. Environ.* **2014**, *148*, 42–57.
42. Congalton, R.G. A comparison of sampling schemes used in generating error matrices for assessing the accuracy of maps generated from remotely sensed data. *Photogramm. Eng. Remote Sens.* **1988**.
43. Reimers, N.; Gurevych, I. Optimal Hyperparameters for Deep LSTM-Networks for Sequence Labeling Tasks. **2017**.
44. Alganci, U.; Ozdogan, M.; Sertel, E.; Ormeci, C. Estimating maize and cotton yield in southeastern Turkey with integrated use of satellite images, meteorological data and digital photographs. *F. Crop. Res.* **2014**, *157*, 8–19.
45. Celik, Y.B.; Sertel, E.; Ustundag, B.B. Identification of corn and cotton fields using multi-temporal Spot6 {NDVI} data. In Proceedings of the 2015 Fourth International Conference on Agro-Geoinformatics (Agro-geoinformatics); IEEE, 2015.
46. Maus, V.; Câmara, G.; Cartaxo, R.; Sanchez, A.; Ramos, F.M.; Ribeiro, G.Q. A Time-Weighted Dynamic Time Warping method for land use and land cover mapping. *IEEE J. Sel. Top. Appl. Earth Obs. Remote Sens.* **2015**, *XX*, 1–10.
47. de Souza, C.H.W.; Mercante, E.; Johann, J.A.; Lamparelli, R.A.C.; Uribe-Opazo, M.A. Mapping and discrimination of soya bean and corn crops using spectro-temporal profiles of vegetation indices. *Int. J. Remote Sens.* **2015**, *36*, 1809–1824.
48. Pan, Z.; Huang, J.; Zhou, Q.; Wang, L.; Cheng, Y.; Zhang, H.; Blackburn, G.A.; Yan, J.; Liu, J. Mapping crop phenology using NDVI time-series derived from HJ-1 A/B data. *Int. J. Appl. Earth Obs. Geoinf.* **2015**, *34*, 188–197.
49. Tang, K.; Zhu, W.; Zhan, P.; Ding, S. An Identification Method for Spring Maize in Northeast China Based on Spectral and Phenological Features. *Remote Sens.* **2018**, *10*, 193.
50. Çopur, O.; Yuka, A. Buğday Sonrası İkinci Ürün Olarak Yetiştirilen Pamuk (*Gossypium hirsutum* L.) Çeşitlerinde Verim ve Verim Unsurlarının Belirlenmesi. *Yüzüncü Yıl Üniversitesi Tarım Bilim. Derg.* **2016**, *26*, 245–253.